Estimation of Lung Properties From the Forced Expiration Data

Adam G. Polak, Dariusz Wysoczański, and Janusz Mroczka

***Abstract*— Forced expiration is the most commonly applied lung function tests. Despite the problem of spirometry modeling was solved a few decades ago, a relatively small amount of work has been devoted to indirect measurements of lung properties from spirometry data. Just recently, a new method, based on the reduced model for forced expiration and two-stage estimation (global with the feed-forward neural network approximating the inverse mapping (InvNN) and then local with the Levenberg–Marquardt algorithm, starting with the rough estimates yielded by the InvNN) was proposed. The aim of this work was to evaluate the accuracy of the above approach to the indirect measurement of lung properties. To this end, 16,000 synthetic spirometry results were generated, and then used to optimize, train, and validate the InvNN, and to test the entire method. The total estimation errors of model parameters were from 3.7% to 16.6% in relation to their variability ranges. Those original estimates were then recalculated to clinically interpretable airway resistances and compliances, assessed with the relative errors of 7%–35% and 5%–12%, respectively. These outcomes encourage the future use of the method to analyze the results of bronchial challenge or dilation tests.**

***Index Terms*— Airway compliance, airway resistance, estimation accuracy, Levenberg–Marquardt (LM) algorithm, neural network, spirometry.**

I. Introduction

SPIROMETRY, and particularly forced expiration, is one of the most commonly applied lung function tests. Its advantages stem from simple and convenient to use measuring equipment, independence of the descending part of flow-volume (FV) curve from patient effort, and from the sensitivity of the FV curve shape to respiratory disorders [1].

In the 1960s and 1970s, the main factors determining the shape of the FV curve were successively identified—first, the role of lung recoil pressure [2], [3], and then the wave-speed flow limiting mechanism in elastic airways [4], [5]. These findings, combined with the morphological model for the symmetrical bronchial tree [6], allowed Lambert and coworkers to elaborate the pioneering, validated, and widely recognized computational model for the descending part of the FV curve [7]. This model was further developed to simulate forced expiration in the whole range of lung vital capacity (VC) [8] and to include the asymmetrical bronchial tree structure [9], [10]. Thereby, the forward problem in spirometry was generally solved.

In metrology, however, the inverse problem takes the central position. In particular, in indirect measurements, it consists in the estimation of properties of an object under investigation based on directly measured data. Such attempts to infer about lung mechanics are currently undertaken in the field of forced oscillations technique [11], mechanical ventilation [12], or computational fluid dynamics [13]. None of these approaches, however, takes into account the elastic properties of bronchi or airflow nonlinearities.

In the case of spirometry, solving the inverse problem means to indirectly measure the lung mechanical properties through advanced FV data processing. Such information would be of great clinical significance. Nevertheless, a relatively small amount of work has been carried out in this field so far, mainly due to the complexity of the respiratory system resulting in sophisticated anatomy- and physiology-based models, as well as advanced data processing techniques to be considered. The first systematic investigations on the sensitivity and specificity of the forward model for forced expiration were performed just after publishing it [14]. This study revealed the main difficulties in its potential use in indirect measurements, such as a large number of parameters, their collinearities, and overall strong functional nonlinearities. Only relatively recently, new attempts were made. The first approach consisted in fitting the model to the descending part of the FV curve by adjusting solely airway maximal areas [15], [16], which represented only a small subset of parameters determining the spirometric data. The second methodology, focused on the parametrization of distribution of specific airway properties along the bronchial tree and the advanced sensitivity analysis, showed that only nine parameters of the reduced model were of metrological meaning [17]. The first comprehensive attempt with this approach was presented just recently, combining the inverse neural network (InvNN) acting as a global estimator with the local Levenberg–Marquardt (LM) estimation method. The obtained total errors of parameter estimates were from 4% to 19% in relation to the parameter variability ranges [18].

The aim of this work was to further improve the abovementioned approach by taking into account other methods of global estimation and better tuning the inherit parameters of the chosen global estimator to show the possibility of translating the estimation results into clinically relevant quantities, as well as to perform comprehensive tests of the entire method for indirect measurement of respiratory system properties.

Manuscript received September 28, 2019; revised January 2, 2020; accepted January 6, 2020. Date of publication January 22, 2020; date of current version May 12, 2020. This work was supported by the National Science Centre, Poland, under Grant 2016/21/B/ST7/02233. The Associate Editor coordinating the review process was Amitava Chatterjee. *(Corresponding author: Adam G. Polak.)*

The authors are with the Chair of Electronic and Photonic Metrology, Faculty of Electronics, Wrocław University of Science and Technology, 50-317 Wrocław, Poland (e-mail: adam.polak@pwr.edu.pl).

Color versions of one or more of the figures in this article are available online at http://ieeexplore.ieee.org.

Digital Object Identifier 10.1109/TIM.2020.2968727

II. Methods

A. Methodology

The typical approach to the identification of complex and nonlinear models consists in solving the optimization problem (i.e., the minimization of the objective function F_{ob}—the distance between the model output and data), and this task should be divided into two stages because of a usually unknown and possibly complex topology of F_{ob}: first—global identification yielding approximate estimates of parameters near the global minimum, and then—a more accurate local estimation method.

First, three methods of global optimization: random search (RS), simulated annealing (SA), and genetic algorithm (GA), were tested as global estimators using the nine-parameter model of normal lung and compared to the performance of the InvNN. Taking into account the obtained results, we decided to continue with the InvNN. The number of free parameters was further decreased to 6 by taking into account the natural optimality of the bronchial tree structure. Then, the synthetic FV data were generated with this model and applied to train the InvNN. The estimates yielded by the InvNN were used as starting points for the LM algorithm of local estimation. The relevant estimates were recalculated into resistances and compliances of airway generations. Finally, the estimates were compared with the true parameter values and their variability ranges, returning the assessments of the relative systematic, random, and total errors of estimation. All the computations and analyses were carried out on a PC with Intel Core i7-6950X CPU at 3.0 GHz, RAM 32 GB, GPU NVIDIA Quadro 8 GB, using MATLAB (R2017a, MathWorks).

B. Forward Model and Its Reduction

The complex forward model for forced expiration, allowing the simulation of the entire spirometric curve, was described elsewhere [8], [19]. Breathily, the model includes the symmetrical bronchial tree with mechanical properties of the airways specified independently for each of their 24 generations. These parameters describe the dependence of the airway lumen area (A) on transmural pressure (P_{tm})

$$A(P_{\mathrm{tm}}) = \begin{cases} A_{\mathrm{m}}\alpha_0(1 - P_{\mathrm{tm}}/P_1)^{-n_1}, & P_{\mathrm{tm}} \le 0 \\ A_{\mathrm{m}}[1-(1-\alpha_0)(1-P_{\mathrm{tm}}/P_2)^{-n_2}], & P_{\mathrm{tm}} > 0 \end{cases} \quad (1)$$

where A_{m} is the maximal airway area, α_0 is the normalized airway area at $P_{\mathrm{tm}} = 0$, α_0' is the slope of α_0 at $P_{\mathrm{tm}} = 0$ (neutral compliance), $P_1 = n_1\alpha_0/\alpha_0'$, $P_2 = n_2(\alpha_0 - 1)/\alpha_0'$, and n_1 and n_2 are the shape-adjusting exponents [7]. The second crucial component is the nonlinear relationship between the elastic recoil pressure (P_{st}) and lung volume (V_{L})

$$P_{\mathrm{st}}(V_{\mathrm{L}}) = \begin{cases} \dfrac{V_{\mathrm{L}} - V_0}{C_{\mathrm{st}}}, & V_{\mathrm{L}} \le V_{\mathrm{tr}} \\ \dfrac{V_{\mathrm{m}} - V_{\mathrm{tr}}}{C_{\mathrm{st}}} \cdot \ln\left(\dfrac{V_{\mathrm{m}} - V_{\mathrm{tr}}}{V_{\mathrm{m}} - V_{\mathrm{L}}}\right) + \dfrac{V_{\mathrm{tr}} - V_0}{C_{\mathrm{st}}}, & V_{\mathrm{L}} > V_{\mathrm{tr}} \end{cases} \quad (2)$$

where V_{L} is the lung volume, V_{m}, V_{tr}, and V_0 are the maximal, transition, and minimal volumes, and C_{st} is the lung compliance defining the linear part of $P_{\mathrm{st}}(V_{\mathrm{L}})$ characteristics [20]. Finally, the airflow Q is computed by repeatedly solving the differential equation for the pressure drop along the lengths l_g of airway generations for a given V_{L} [7]

$$\frac{dP}{dx} = \frac{f_{\mathrm{d}}(x)}{1 - \frac{u^2(x)}{c^2(x)}} = \frac{f_{\mathrm{d}}(x)}{1 - \frac{\rho Q^2}{A^3(x)}\left(\frac{\partial A}{\partial P_{\mathrm{tm}}}\right)_x} \quad (3)$$

where dP/dx is the gradient of pressure along a bronchus, u and c are the local airflow and wave speeds, ρ is the gas density, and

$$f_{\mathrm{d}}(x) = (a + b \cdot \mathrm{Re}(Q, x)) \cdot \frac{8\pi\mu Q(x)}{A^2(x)} \quad (4)$$

is the elementary dissipative pressure loss at the point x (a and b are the proportionality coefficients, Re is the local Reynolds number, and μ is the gas viscosity) [21]. Each time, the total pressure drop along the airways is equated to the instant driving pressure to find actual Q.

The first stage of the systematic reduction of that forward model was achieved by replacing a great number of its original parameters by functions that describe the distributions of airway properties (such as A_{m}, α_0', or α_0) along the bronchial tree, as well as by considering the uninfluential parameters as constants (based on the sensitivity analysis of the descending part of the FV curve, which is determined by the mechanism of flow limitation). This model had nine parameters, all accompanied by the ranges of their variability [17]. However, one of the basic features characterizing the bronchial tree has not been included in that reduced model—namely, the natural optimality of its structure, manifesting in fixed ratios between linear dimensions (diameters and lengths) of subsequent airway generations [22], [23]. This means that the intersubject variability (approximately ±30% [24]–[26]) in lung dimensions may be captured by one scaling parameter, p_{l}. Thus, the structural parameters of an individual subject, l_g and A_{m} (unaffected by airway remolding and narrowing [19]), have been related to p_{l} in this study. Moreover, it is obvious that two other airway properties do not change independently during the constriction of airway smooth muscle: the resulting lumen area (related to α_0) and wall compliance (related to α_0') [19], [27]. Using the reported relationships between the airway diameter, wall thickness, and compliance [28], [29], another scaling parameter, k_a, has been used in the model to describe the effects of airway narrowing, such that when α_0 alters proportionally to k_a, α_0' changes in proportion to k_a^2. This relationship is in line with experimental results [19]. Because the specific level and location of airway constriction is generally unknown, its distribution along the bronchial tree is finally expressed by the sigmoidal function with two parameters, p_{a1} and p_{a2}

$$k_a(g) = \frac{0.0196 \cdot g + 1.05}{1 + \exp(p_{a1}g + p_{a2})} - 0.0174 \cdot g + 0.7 \quad (5)$$

where g denotes the airway generation. Modifications of p_{a1} and p_{a2} allow for alternative simulations of: unchanged properties, homogeneous alterations, or dominant modifications in the zone of small or big airways. Considering various published results, the coefficients in (5) have been chosen in such a way that the sigmoidal upper asymptote varies between

TABLE I
FREE PARAMETERS OF THE REDUCED MODEL AND THE ASSESSED RANGES OF THEIR VARIABILITY

Ranges of variability	Parameter					
	p_l	p_{a1}	p_{a2}	ΔV_0	ΔV_{tr}	C_{st}
Lower limit	0.7	–0.19	0.92	–0.5	0.0	2
Upper limit	1.3	0.16	3.4	0.0	VC–0.5	10

VC – vital capacity; volumes in dm^3, lung compliance C_{st} in $dm^3 \cdot kPa^{-1}$

1.05 for $g = 0$ (the modified α_0 cannot exceed 1) and 1.5 for $g = 23$, and the lower asymptote between 0.7 for $g = 0$ (stiffer airways) and 0.3 for $g = 23$ (resulting in approximately 120 times increased resistance of these airways). Ranges of p_{a1} and p_{a2} have been assessed to keep k_a within 5%–95% of these asymptotes. The last step of model reduction was moving V_{m} from the set of free parameters to constants (using its approximate relation to the total lung capacity: $V_{\mathrm{m}} = 1.05 \cdot \mathrm{TLC}$), because it modifies only the last part of $P_{\mathrm{st}}(V_{\mathrm{L}})$ characteristics related to maximal lung volumes, and the relevant data (the ascending part of the FV curve) will not be used when identifying the model. In addition, the volumetric parameters from the $P_{\mathrm{st}}(V_{\mathrm{L}})$ characteristics, V_0 and V_{tr}, were referenced to the lung residual volume (insignificant parameter), so they are denoted as ΔV_0 and ΔV_{tr} in the reduced model. The six parameters of the reduced model are collected in Table I together with their ranges of variability.

C. Preliminary Tests of Global Optimization Methods

Just recently, an analogous model was used to create and evaluate a feed-forward neural network (FFNN) approximating the inverse mapping between the spirometric data and model parameters (InvNN). This approach has been considered because any multidimensional continuous mapping can be arbitrary well approximated using the FFNN [30], [31].

The total relative error of estimation of individual parameters using this InvNN was between 11% and 28% (dominated by estimate deviations) of their variability ranges [32]. Further attempts based on this inverse mapping have shown that it often returns parameter estimates characterizing local minima of F_{ob}, giving an inadequate solution to the inverse problem in such cases. To continue with possibly the best approach to global estimation, three other methods for stochastic optimization were tested and compared to the results of InvNN: RS, SA, and GA. These methods were chosen because of their similarities, popularity, and the ability of easily imposing bounds on parameters. The simplest one is RS with an iteratively damped region of interest, where the next population of analyzed points is drawn around the best parameter vector found in the previous step. On the contrary, in SA only one evaluation of F_{ob} is done in a new random direction per one iteration with the decreasing step and with the possibility of accepting worse solutions. The most advanced is GA, mimicking biological evolution when creating new descendant populations of parameters. For each algorithm, the same maximal number of F_{ob} evaluations, fitness limit, and the population size in RS and GA was set. The methods were tested using FV data generated by the nine-parameter model. Identifications were performed 30 times for each method to assess statistical features of the algorithms: mean errors and standard deviations (SDs) of parameter identification, both related to the parameter variability ranges.

D. Generation of Synthetic Data

The preliminary tests revealed InvNN's advantage as a global estimator, nonetheless, using it required a huge amount of spirometric data related to specific parameters of the reduced model and appropriate choice of InvNN features.

The former was achieved by a synthetic generation of 16,000 FV curves representing a variety of possible states of the respiratory system. In the beginning, the sex of a virtual subject was randomly chosen as female (F) or male (M). Then, its height and age were randomly drawn (uniform distribution) from the ranges 1.50–1.80 (F) or 1.60–1.90 cm (M), and 25–70 years, respectively. These data were used to calculate the predicted values of VC and other basic spirometric indices characterizing this subject, such as forced expiration volume in 1 s (FEV_1), Tiffeneau index ($\mathrm{FEV}_1/\mathrm{FVC}$), forced mid-expiratory flow between 25% and 75% of FVC ($\mathrm{FEF}_{25\%-75\%}$), and peak expiratory flow (PEF) [33]. Then, the whole FV curve was simulated in the range of VC (100 evenly spread samples) using the values of model parameters (the target vector for the InvNN) randomly drawn from their variability ranges (uniform distribution). Finally, the first volume after PEF ($V_{\max}$) was found and 100 samples of the descending part, evenly distributed between $V_{\max}$ and VC, were computed again. The simulated flow data were then supplemented with the values of $V_{\max}$ and VC, forming the input vector for the InvNN. Because some combinations of randomly chosen parameter values were returning unnatural FV curves, additionally the spirometric indices were calculated from the simulated data and compared with the upper 95 percentiles of the predicted values for that subject [33]. When any of these limits was exceeded or the volume corresponding to PEF was smaller than 6% of VC, such an FV curve was rejected. In the end, the flow data were corrupted with white noise, by adding random samples from the normal distribution, with an SD of 0.01 $\mathrm{dm}^3 \cdot \mathrm{s}^{-1}$ deduced from the available spirometric sensor connected to the data acquisition system [32]. The above procedure yielded the sets of corresponding input ($102 \times 16{,}000$) and target ($6 \times 16{,}000$) data.

E. Global Estimation Using the InvNN

To decide about the InvNN preferred features, preliminary studies on the inverse mapping quality were carried out with: 1) 8,000 versus 16,000 sets of FV curves; 2) 52 versus 102 data in an FV set; 3) LM versus scaled conjugate gradient (SCG) training methods; and 4) tansig versus logsig activation functions—all analyses were done with different numbers of neurons in two hidden layers (from 20, every 10, to 50) and 30 initializations of each InvNN. Finally (see Section III), the InvNN with 102 input neurons, two hidden layers with 40 neurons each (with logsig activation functions), and 6 linear

output neurons were trained using the LM method, with the initial value of the regularization parameter equal to 10^{-3}.

All artificially generated data were divided into the training, validation, and test sets, in the proportion 0.7:0.15:0.15 (11,200:2,400:2,400 elements). The input data were left in their original ranges. On the other hand, the absolute values of parameters differed from each other by several orders, so the target data (expected parameter values) were scaled by their ranges of variability (Table I). Additionally, the formerly assessed error weights [5 2 1 3 8 3] were assigned to the corresponding InvNN outputs to enhance the accuracy of estimation of the most significant parameters [32]. The validation set was used to stop training before overfeeding the network (after ten unsuccessful steps), with a network performance evaluated by the mean squared error (MSE). The InvNN structure that yielded the least MSE for the validation set was further trained 100 times, and the one characterized by the smallest MSE was ultimately considered the best achieved inverse mapping between the spirometric data and the parameters of the reduced model. The first estimates of parameters were computed using this InvNN and the FV curves from the test set. Since the InvNN implements the continuous inverse mapping, some estimates may fall outside the feasible ranges. For this reason, such estimates were corrected using the limits given in Table I.

F. Local Estimation Using the LM Method

The final stage of inverse problem solving involved local estimation, starting from the rough estimates yielded by the InvNN. The sensitivity analysis of the reduced model done for a set of typical respiratory system states [32] had revealed that the gradient-based procedures of local estimation may be numerically ill-conditioned (coefficients of Pearson correlation between sensitivity vectors sometimes higher than 0.999). This caused that the LM method was chosen to iteratively find the estimates of model parameters $\hat{\boldsymbol{\theta}}$ by minimizing the distance between the model output $\mathbf{Q}_{\mathrm{m}}(\boldsymbol{\theta})$ and flow data $\mathbf{Q}$. The LM algorithm balances between the steepest descent and Gauss–Newton directions of minimum search by modifying the regularization parameter λ according to the local topology of F_{ob}, and simultaneously avoids the ill-conditioning of matrix inversion by adding small λ values to its diagonal

$$\hat{\boldsymbol{\theta}}_{i+1} = \hat{\boldsymbol{\theta}}_i + \mu\left(\mathbf{X}_i^{\mathrm{T}}\mathbf{X}_i + \lambda_i \mathbf{I}\right)^{-1}\mathbf{X}_i^{\mathrm{T}}\boldsymbol{\varepsilon}_i \tag{6}$$

where the sensitivity matrix (computed numerically) $\mathbf{X} = \partial\mathbf{Q}_{\mathrm{m}}/\partial\boldsymbol{\theta}$, the residues $\varepsilon = \mathbf{Q} - \mathbf{Q}_{\mathrm{m}}$, and μ is the step size (0.5 in this study). In addition, this iterative routine attracts poorly defined estimates to their previous values, so it preserves the values of such parameters that have been used in the starting vector (resulting from global estimation) [34]. In the original LM method, λ is tuned based on the model fit to data, which is not the best approach in indirect measurements, where a method should focus on the accuracy of parameter estimates. Thus, recently an alternative approach was proposed to modify λ, assessing the balance between the systematic and random error of estimation in each iteration [34]. This is done by calculating values of the auxiliary variable V_λ for $\lambda_{i+1} = 10 \cdot \lambda_i$, $\lambda_{i+1} = \lambda_i$ and $\lambda_{i+1} = \lambda_i/10$. V_λ consists of two terms, related, respectively, to the systematic and random errors

$$V_\lambda = \boldsymbol{\varepsilon}^{\mathrm{T}}(\lambda_{i+1})\boldsymbol{\varepsilon}(\lambda_{i+1}) + \hat{\boldsymbol{\sigma}}_\theta^{\mathrm{T}}(\lambda_{i+1})\mathbf{X}^{\mathrm{T}}\mathbf{X}\hat{\boldsymbol{\sigma}}_\theta(\lambda_{i+1}) \tag{7}$$

where $\hat{\boldsymbol{\sigma}}_\theta$ is a vector of SDs of parameter estimates assessed by cross-validation (leave-one-out), Eventually, such λ_{i+1} is selected for use in the next iteration, which returns the minimal V_λ.

The above algorithm, taking additionally into account constraints on the estimates given by the lower and upper parameter bounds (Table I), was applied to calculate the final estimates of model parameters.

G. Calculation of Clinically Interpretable Parameters

The derived reduced model has six free parameters, where three of them correspond to airway mechanics, and the other three to the elastic properties of lung tissue. The only clinically recognized parameter from this set is lung compliance C_{st} [see (2)]. Simultaneously, very important information on the airway state is encoded in the parameters p_{a1} and p_{a2}, which describe the distribution of airway narrowing along the bronchial tree (5). Fortunately, these parameters can be recalculated into well-established in clinical practice resistances and compliances of airway generations for the conditions characterizing the end of normal expiration, when cross sections of flexible airways are constant due to a very small airflow Q, and typical $P_{\mathrm{tm}} = 0.5$ kPa, so [see (3) and (4)]

$$\frac{dP}{dx} = \frac{a8\pi\mu Q}{A^2} \Rightarrow \Delta P = \int_0^{\mathrm{l}_g} \frac{a8\pi\mu Q}{A^2}dx = \frac{a8\pi\mu Q \mathrm{l}_g}{A^2} \tag{8}$$

where the length of an airway generation, l_g, depends on parameter p_{l}. Then the resistance R_g of 2^g parallel airways in generation g is equal to

$$R_g(g) = \frac{1}{2^g}\frac{\Delta P}{Q} = \frac{a8\pi\mu \mathrm{l}_g}{2^g A^2}. \tag{9}$$

Analogously, the compliance of parallel airways can be derived from (1) according to its definition as follows:

$$\begin{aligned} C_g(g) &= 2^g \frac{\partial V_{aw}}{\partial P_{\mathrm{tm}}} = 2^g \mathrm{l}_g \frac{\partial A}{\partial P_{\mathrm{tm}}} \\ &= 2^g \mathrm{l}_g A_{\mathrm{m}}(\alpha_0 - 1)\frac{n_2}{P_2}\left(1 - \frac{P_{\mathrm{tm}}}{P_2}\right)^{-n_2-1} \end{aligned} \tag{10}$$

where V_{aw} is the airway volume, and A_{m}, α and P_2 depend on p_{l}, p_{a1}, and p_{a2}.

H. Metrological Analysis of Results

The accuracy of estimation performed by the InvNN and LM methods was evaluated using the test set of synthetic data (with 2,400 elements composed of true parameter vectors $\boldsymbol{\theta}^*$ and corresponding FV curves). Because the true values of parameters were known, it was straightforward to calculate the relative error of estimation for each parameter, taking into account the range of its variability r (see Table I)

$$\delta\theta_k = \left(\hat{\theta}_k - \theta_k^*\right)/r_k. \tag{11}$$

Such an approach to expressing the relative error seems better than the classical one, $\delta\theta = (\hat{\theta} - \theta^*)/\theta^*$, when the true

TABLE II

ASSESSED RELATIVE ACCURACY OF ESTIMATION WITH THE INVNN AND LM ALGORITHMS

Relative errors of estimation (%)		Estimated parameter					
		p_l	p_{a1}	p_{a2}	ΔV_0	ΔV_{tr}	C_{st}
InvNN	d_m	–0.07	0.13	–0.47	–0.01	–0.07	–0.19
	d_s	4.58	7.73	16.63	4.54	3.84	5.11
	d_t	4.58	7.73	16.64	4.54	3.84	5.11
LM	d_m	–0.03	0.29	–0.58	0.33	0.68	–0.68
	d_s	3.67	6.53	16.54	3.83	4.16	4.10
	d_t	3.67	6.53	16.55	3.84	4.22	4.15

d_m – mean errors, d_s – standard deviations of errors, and d_t – total errors

value can be 0, as in this study. Having $N = 2{,}400$ estimates of each parameter, the statistical characteristics of relative errors could be evaluated—the mean error $\mathrm{d_m}$, the SD of errors $\mathrm{d_s}$, and the total error $\mathrm{d_t}$, as follows:

$$\mathrm{d_m}(k) = \frac{1}{N}\sum_{i=1}^{N}\delta\theta_k$$

$$\mathrm{d_s}(k) = \sqrt{\frac{1}{N-1}\sum_{i=1}^{N}(\delta\theta_k - \mathrm{d_m}(k))^2}$$

$$\mathrm{d_t}(k) = \sqrt{\mathrm{d_m^2}(k) + \mathrm{d_s^2}(k)}. \quad (12)$$

With the true values of model parameters and their estimates, it is also possible to find relative errors of R_g and C_g calculated on their basis for each airway generation

$$\delta R_g = \left(\hat{R}_g - R_g^*\right)/R_g^*, \quad \delta C_g = \left(\hat{C}_g - C_g^*\right)/C_g^*. \quad (13)$$

III. RESULTS

The results of global estimations using RS, SA, and GA revealed large mean errors and their SDs, ranging from 0.2% to 27.6% (mean) and 2.4% to 33.1% (SD), depending on a method and parameter. They were larger than the errors yielded by the InvNN (Table II). Moreover, these computations required a huge number of F_{ob} evaluations: $(5.4 \pm 4.3) \times 10^3$, $(7.0 \pm 1.5) \times 10^3$, and $(2.7 \pm 1.5) \times 10^4$, respectively, prolonging the first stage of estimation.

Investigation on the preferred features of the InvNN returned some expected outcomes: the errors of estimation were smaller for 16,000 versus 8,000 sets of FV curves, and 102 versus 52 input data, as well some additional information: using SCG backpropagation significantly worsened the accuracy compared to the LM algorithm, and the logsig activation function improved slightly the accuracy of global estimation compared to tansig.

Based on the above results, a large ensemble of synthetic data was generated, consisting of 16,000 vectors of model parameters and corresponding spirometric curves. Examples of the test data are presented in Fig. 1.

The first portion of these data (11,200 training and 2,400 validation elements) was used to train and optimize the InvNN with 40 neurons in each of the two hidden layers. This InvNN was further used as a global estimator and evaluated with the test data (remaining 2,400 elements). The results of this stage, in terms of estimation errors, are shown in the top panel of Table II. Then, the estimates returned by the InvNN (corrected when necessary to be within the parameter ranges, which sometimes worsen the model fit) were used as starting vectors for local estimation with the LM. An example of improving the model fit to the descending part of a spirometric curve is shown in Fig. 2, and the relationships between the final estimates and true parameter values in Fig. 3.

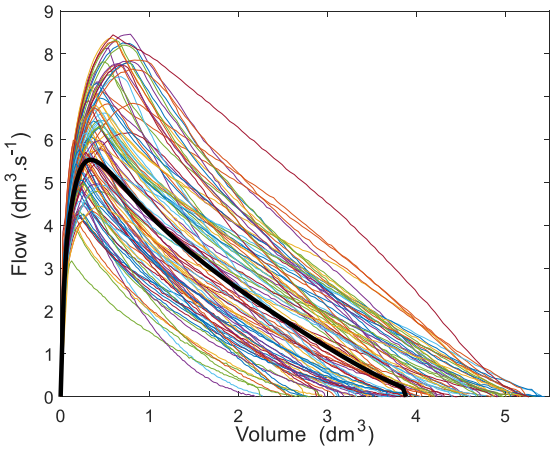

Fig. 1. First 100 spirometric curves from the test set (thin lines) and the main trend from the whole set (bold line).

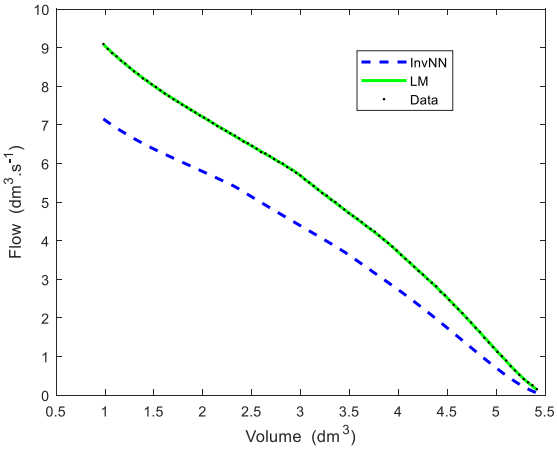

Fig. 2. Fit of the reduced model to spirometric data in the case of the worst-matched InvNN model.

The final errors of this stage of estimation are collected in the low panel of Table II. These results reveal that the most accurately assessed parameter is p_{l} (3.7% of the variability range)—responsible for scaling the linear dimensions of airways, and the less accurately assessed is p_{a2} (16.6%)—describing the homogeneous narrowing/dilating of all airway generations (5). The final stage using the LM method has improved the accuracy of all parameter estimates, but ΔV_{tr}.

Upon inspecting the results of R_g and C_g assessment shown in Fig. 4, it is apparent that retrieving airway compliances from spirometric data is more accurate than extracting airway resistances (total errors of 5%–12% versus 7%–35%), and that accuracy is three–four times better for large bronchi (first airway generations) than that for small bronchioli (last generations). Simultaneously, the third clinically

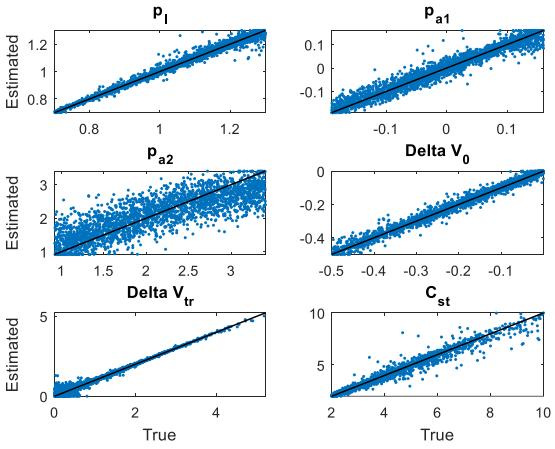

Fig. 3. Dependencies between estimated and true values of model parameters with the identity lines (see Table I for definitions).

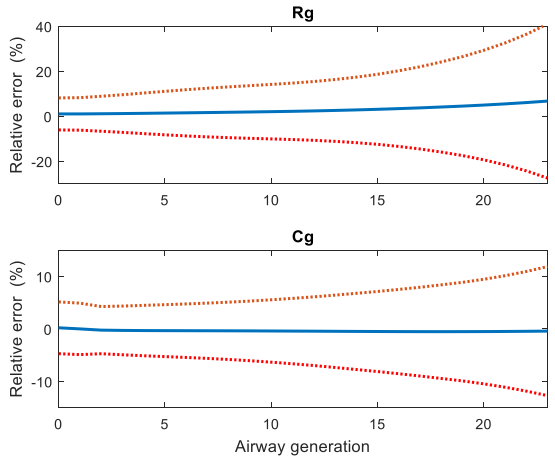

Fig. 4. Distribution of relative estimation errors (mean ± SD) of airway resistances and compliances along the bronchial tree generations.

valuable parameter, C_{st}, is directly estimated with a relatively small error of 4.2% (Table II).

IV. Discussion

The aim of this work was to evaluate the effectiveness of the proposed method for indirect measurement of respiratory system properties based on the reduced model for forced expiration, including the stages of global and local estimation.

The reduction of the complex model for forced expiration has been performed by analyzing only the descending part of the spirometric curve, taking into account the natural optimality of the bronchial tree structure, describing the distribution of airway properties along their generations with the scaling function, and treating the least influential parameters as constants. Nevertheless, the computational structure of the reduced model has not been changed and it is fully compliant with the complex model, i.e., it includes all the essential relationships. According to our best knowledge, this is the first compact (in terms of free parameters), yet still rational model (in terms of respiratory anatomy and physiology/ pathophysiology) that has been proposed to solve the inverse problem in spirometry.

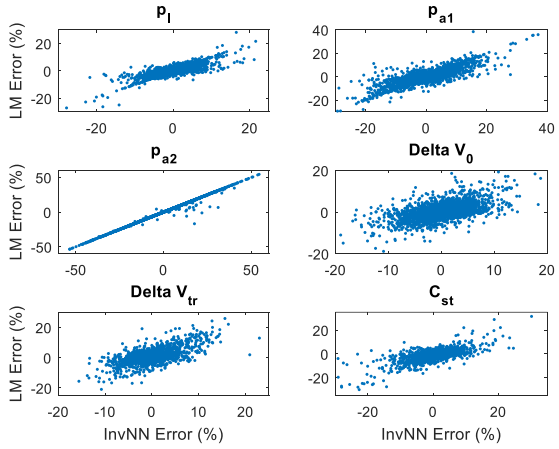

Fig. 5. Dependencies between LM and InvNN estimation errors.

After the tests with a few methods of global optimization, the FFNN approximating the inverse mapping between spirometric data and model parameters (InvNN) was chosen as returning more accurate estimates. Although the time of its training is quite long and comparable to RS, SA, or GA, the evaluation of model parameters from new data is very fast, substantially shortening the stage of global estimation, which makes that this approach outweighs the others in the contest of clinical application. Considering the InvNN training, the LM backpropagation algorithm has outperformed the SCG method, which follows two facts. First, the sought inverse mapping is numerically ill-conditioned (strong correlations between model parameters), so the LM approach is recommended [34]. In addition, the SCG algorithm has been run on the GPU that uses single-precision arithmetic with rounding being destructive in the case of ill-conditioned problems.

All the analyses were done based on the test data, never used at the stage of InvNN training and optimization. The main results are collected in Table II. Small vales of $\mathrm{d_m}$ prove that systematic errors (caused mainly by the regularization mechanism and the stop criterion in the iterative LM algorithm) are negligible compared to the random errors represented by $\mathrm{d_s}$. The $\mathrm{d_s}$ have a major contribution to the expected total errors of estimation ($\mathrm{d_t}$). These, sometimes fairly large values (above 16% for p_{a2}), result mainly from the presence of noise in the data, the relatively small sensitivity of the model output to some parameters and the high correlation between the impact of certain parameters (mainly between p_{l} and p_{a2}, and p_{a2} and C_{st}). This effect is well visible in Fig. 3, where the dispersion of p_{a2} estimates is much bigger than, e.g., those of p_{l}. The estimation procedure consists of two stages and the LM estimates are computed starting from the InvNN ones. This results in a strong linear correlation of LM on InvINN estimates of parameters weakly defined by the data (Fig. 5), particularly in the case of p_{a2}, ($r^2 = 0.993$ versus 0.328 for ΔV_0), and in the inability of the second algorithm to significantly improve the results. Summarizing, the relatively unprecise estimation of p_{a2} follows its weak identifiability, shown also by the sensitivity analysis of the reduced model. On the other hand, it could not be removed from the set of free parameters, having a much greater impact on the model

output compared to the parameters treated as constants in the reduced model. In general, the high correlations cause that an inaccurate match of one parameter can be almost completely compensated by the changed value of another, and the model still fits the data very well—as in Fig. 2. From Table II, it also stems that some of the InvNN estimates do not lie close to the global minimum, which is a feature of most global estimation methods. Another finding worth to note is that the best (for ΔV_{tr}) and worst (for p_{a2}) InvNN estimation accuracy is well related to the *a priori* assessed error weights: 8 and 1, respectively.

The errors of directly estimated parameters translate into inaccuracy of the assessment of airway resistance and compliance distribution along the bronchial tree (Fig. 4). This evaluation is fairly precise for large airways, but it falls toward the lung periphery. The lower sensitivity of measurement results in changes in the small airways observed here is well known and referred to as the "silent zone" effect [35]. Nevertheless, the proposed approach is currently the only one allowing the noninvasive assessment of the airway resistance and compliance distribution along the bronchial tree.

The above discussed disadvantages could be avoided by taking into account outcomes from other medical examinations, such as computed tomography (to assess p_{l}) [36] or measurements with an esophageal balloon (to estimate independently ΔV_0, ΔV_{tr}, and C_{st}) [20]—but this is not part of the clinical routine. However, there is one more possibility, relevant to clinical concern, to reduce the errors resulting from large correlations between parameter estimators, associated with a further reduction in the number of free model parameters. The principle of differential measurements, eliminating systematic errors produced by unmeasured variables, can be applied to data from two spirometric examinations, representing the same patient with only changed airway properties (represented by p_{a1} and p_{a2}), as in bronchial dilation or challenge tests.

The analysis of estimation based on data generated in advance by the same model is usually referred to as inverse crime [37]. On the other hand, as long as the desirable properties of any new inversion method have not been proven in this sometimes trivial case, there is no point in using it with other data, including experimental measurements. In this study, however, the synthetic data were corrupted by realistic white noise, which allowed to assess its impact on estimate variances (random errors), as well as to compare this effect with the bias resulting from regularization (systematic errors). Nevertheless, it is planned to use spirometry data of another origin in the future, including spirometric curves generated by the computational model with heterogeneous bronchial tree [38].

V. Conclusion

The main contribution of this study covers the following issues. First, the maximally compact in terms of free parameters, however capturing the main properties of the respiratory system, reduced model for forced expiration was proposed. Then the procedure for identifying this nonlinear model, including the global and local stages, was shown. We also presented how to recalculate the estimates of model parameters into the distributions of clinically interpretable airway resistances and compliances. Finally, the metrological properties of the above approach to solving the inverse problem in spirometry were assessed. The possibility of noninvasive insight into the airway and lung tissue mechanics, only by additionally processing data from popular spirometry tests (without any interference with the expiration procedure and spirometers hardware), is of great innovative and clinical significance. The future study will focus on using this methodology in the differential measurement of changes in airway properties (represented by p_{a1} and p_{a2}) based on two spirometric examinations, recorded during bronchial challenge or dilation tests.

References

[1] R. Pellegrino, "Interpretative strategies for lung function tests," *Eur. Respiratory J.*, vol. 26, no. 5, pp. 948–968, Nov. 2005.

[2] J. Mead, J. M. Turner, P. T. Macklem, and J. B. Little, "Significance of the relationship between lung recoil and maximum expiratory flow," *J. Appl. Physiol.*, vol. 22, no. 1, pp. 95–108, Jan. 1967.

[3] N. B. Pride, S. Permutt, R. L. Riley, and B. Bromberger-Barnea, "Determinants of maximal expiratory flow from the lungs," *J. Appl. Physiol.*, vol. 23, no. 5, pp. 646–662, Nov. 1967.

[4] S. V. Dawson and E. A. Elliott, "Wave-speed limitation on expiratory flow-a unifying concept," *J. Appl. Physiol.*, vol. 43, no. 3, pp. 498–515, Sep. 1977.

[5] A. H. Shapiro, "Steady flow in collapsible tubes," *J. Biomech. Eng.*, vol. 99, no. 3, pp. 126–147, Aug. 1977.

[6] E. R. Weibel, *Morphometry of the Human Lung*. New York, NY, USA: Academic, 1963.

[7] R. K. Lambert, T. A. Wilson, R. E. Hyatt, and J. R. Rodarte, "A computational model for expiratory flow," *J. Appl. Physiol.*, vol. 52, no. 1, pp. 44–56, Jan. 1982.

[8] A. G. Polak, "A forward model for maximum expiration," *Comput. Biol. Med.*, vol. 28, no. 6, pp. 613–625, Nov. 1998.

[9] A. G. Polak and K. R. Lutchen, "Computational model for forced expiration from asymmetric normal lungs," *Ann. Biomed. Eng.*, vol. 31, no. 8, pp. 891–907, Sep. 2003.

[10] K. L. Hedges, A. R. Clark, and M. H. Tawhai, "Comparison of generic and subject-specific models for simulation of pulmonary perfusion and forced expiration," *Interface Focus*, vol. 5, no. 2, Apr. 2015, Art. no. 20140090.

[11] P. Ghafarian, H. Jamaati, and S. M. Hashemian, "A review on human respiratory modeling," *Tanaffos*, vol. 15, no. 2, pp. 61–69, 2016.

[12] J. Niu *et al.*, "Study on air flow dynamic characteristic of mechanical ventilation of a lung simulator," *Sci. China Technol. Sci.*, vol. 60, no. 2, pp. 243–250, Feb. 2017.

[13] R. R. Kannan, N. Singh, and A. Przekwas, "A quasi-3D compartmental multi-scale approach to detect and quantify diseased regional lung constriction using spirometry data," *Int. J. Numer. Methods Biomed. Eng.*, vol. 34, no. 5, p. e2973, May 2018.

[14] R. K. Lambert, "Sensitivity and specificity of the computational model for maximal expiratory flow," *J. Appl. Physiol.*, vol. 57, no. 4, pp. 958–970, Oct. 1984.

[15] R. K. Lambert, R. G. Castile, and R. S. Tepper, "Model of forced expiratory flows and airway geometry in infants," *J. Appl. Physiol.*, vol. 96, no. 2, pp. 688–692, Feb. 2004.

[16] R. K. Lambert and K. C. Beck, "Airway area distribution from the forced expiration maneuver," *J. Appl. Physiol.*, vol. 97, no. 2, pp. 570–578, Aug. 2004.

[17] J. Mroczka and A. G. Polak, "Selection of identifiable parameters from the reduced model for forced expiration," in *Proc. World Congr. Med. Phys. Biomed. Eng.*, vol. 14, J. Nagel and R. Magjarevic, Eds. Berlin, Germany: Springer, 2006, pp. 664–667.

[18] A. G. Polak, D. Wysoczanski, and J. Mroczka, "Solving the inverse problem in spirometry with the methods of global and local estimation," in *Proc. IEEE Int. Symp. Med. Meas. Appl. (MeMeA)*, Istanbul, Turkey, Jun. 2019, pp. 1–6.

[19] B. Morlion and A. Polak, "Simulation of lung function evolution after heart-lung transplantation using a numerical model," *IEEE Trans. Biomed. Eng.*, vol. 52, no. 7, pp. 1180–1187, Jul. 2005.

[20] J. M. Bogaard *et al.*, "Pressure-volume analysis of the lung with an exponential and linear-exponential model in asthma and COPD. Dutch CNSLD study group," *Eur. Respir. J.*, vol. 8, no. 9, pp. 1525–1531, Sep. 1995.
[21] D. B. Reynolds, "Steady expiratory flow-pressure relationship in a model of the human bronchial tree," *J. Biomech. Eng.*, vol. 104, no. 2, pp. 153–158, May 1982.
[22] B. Mauroy, M. Filoche, E. R. Weibel, and B. Sapoval, "An optimal bronchial tree may be dangerous," *Nature*, vol. 427, no. 6975, pp. 633–636, Feb. 2004.
[23] E. Lee, M. Y. Kang, H. J. Yang, and J. W. Lee, "Optimality in the variation of average branching angle with generation in the human bronchial tree," *Ann. Biomed. Eng.*, vol. 36, no. 6, pp. 1004–1013, Jun. 2008.
[24] M. S. Hannallah, J. L. Benumof, and U. E. Ruttimann, "The relationship between left mainstem bronchial diameter and patient size," *J. Cardiothoracic Vascular Anesthesia*, vol. 9, no. 2, pp. 119–121, Apr. 1995.
[25] A. Majumdar *et al.*, "Relating airway diameter distributions to regular branching asymmetry in the lung," *Phys. Rev. Lett.*, vol. 95, no. 16, Oct. 2005, Art. no. 168101.
[26] D. Kim, J.-S. Son, S. Ko, W. Jeong, and H. Lim, "Measurements of the length and diameter of main bronchi on three-dimensional images in Asian adult patients in comparison with the height of patients," *J. Cardiothoracic Vascular Anesthesia*, vol. 28, no. 4, pp. 890–895, Aug. 2014.
[27] R. H. Brown and W. Mitzner, "Effect of lung inflation and airway muscle tone on airway diameter *in vivo*," *J. Appl. Physiol.*, vol. 80, no. 5, pp. 1581–1588, May 1996.
[28] B. Suki, R. H. Habib, and A. C. Jackson, "Wave propagation, input impedance, and wall mechanics of the calf trachea from 16 to 1,600 Hz," *J. Appl. Physiol.*, vol. 75, no. 6, pp. 2755–2766, Dec. 1993.
[29] H. L. Gillis and K. R. Lutchen, "How heterogeneous bronchoconstriction affects ventilation distribution in human lungs: A morphometric model," *Ann. Biomed. Eng.*, vol. 27, no. 1, pp. 14–22, Jan. 1999.
[30] K. Hornik, "Approximation capabilities of multilayer feedforward networks," *Neural Netw.*, vol. 4, no. 2, pp. 251–257, 1991.
[31] H. Kabir, Y. Wang, M. Yu, and Q.-J. Zhang, "Neural network inverse modeling and applications to microwave filter design," *IEEE Trans. Microw. Theory Techn.*, vol. 56, no. 4, pp. 867–879, Apr. 2008.
[32] A. G. Polak, D. Wysoczański, and J. Mroczka, "Estimation of lung properties using ANN-based inverse modeling of spirometric data," in *Proc. 7th Int. Work-Conf. Bioinform. Biomed. Eng.*, Spain, May 2019, pp. 561–572.
[33] P. H. Quanjer, G. J. Tammeling, J. E. Cotes, O. F. Pedersen, R. Peslin, and J. C. Yernault, "Lung volumes and forced ventilatory flows," *Eur. Respir. J.*, vol. 6, no. 16, pp. 5–40, Mar. 1993.
[34] A. Polak, "An error-minimizing approach to regularization in indirect measurements," *IEEE Trans. Instrum. Meas.*, vol. 59, no. 2, pp. 379–386, Feb. 2010.
[35] J. Mead, "The lung's quiet zone," *New England J. Med.*, vol. 282, no. 23, pp. 1318–1319, Jun. 1970.
[36] S. Miyawaki, M. H. Tawhai, E. A. Hoffman, S. E. Wenzel, and C.-L. Lin, "Automatic construction of subject-specific human airway geometry including trifurcations based on a CT-segmented airway skeleton and surface," *Biomech. Model. Mechanobiol.*, vol. 16, no. 2, pp. 583–596, Apr. 2017.
[37] C. E. Chávez, F. Alonzo-Atienza, and D. Alvarez, "Avoiding the inverse crime in the inverse problem of electrocardiography: Estimating the shape and location of cardiac ischemia," *Comput. Cardiol.*, vol. 40, pp. 687–690, Sep. 2013.
[38] A. G. Polak, D. Wysoczański, and J. Mroczka, "Effects of homogeneous and heterogeneous changes in the lung periphery on spirometry results," *Comput. Methods Programs Biomed.*, vol. 173, pp. 139–145, May 2019.

Adam G. Polak received the M.Sc., Ph.D., and D.Sc. degrees in technical sciences from the Wrocław University of Science and Technology (WUST), Wrocław, Poland, in 1988, 1994, and 2008, respectively.

In 1992 and 1993, he held a fellowship at the British Council, City University, London, U.K. He is currently an Associate Professor with WUST. His research includes indirect measurements, the regularization of parameter estimation and signal reconstruction, modeling and measurements in physiology (particularly respiratory system's properties), the reconstruction of computed tomography (CT) images, and machine learning in disease detection.

Dr. Polak was a recipient of the awards of the Foundation for Polish Science in 1995, the Department IV of the Polish Academy of Sciences (PAS) in 2008, and the scholarship Enhancing Science Linkages Between New Zealand and Europe Through Poland in 2010. He is a member of the Committee on Metrology and Scientific Instrumentation, PAS. Since 2018, he has been serving as an Associate Editor for the IEEE TRANSACTIONS ON INSTRUMENTATION AND MEASUREMENT.

Dariusz Wysoczański received the M.Sc. degree from the Faculty of Electronics, Wrocław University of Science and Technology (WUST), Wrocław, Poland, in 1992, and the Ph.D. degree from the Faculty of Sciences, University of Rouen, Mont-Saint-Aignan, France (co-tutelle Polish-French), in 1996.

He is currently an Assistant Professor with WUST. His research includes indirect measurements, control and measuring microprocessor systems, the application of scattered light in measurements, multiple light scattering modeling, image reconstruction in tomography, and measuring methods and techniques.

Dr. Wysoczański was a recipient of the Award of the Foundation for Polish Science in 1999.

Janusz Mroczka received the M.Sc., Ph.D., and D.Sc. (habilitation) degrees from the Wrocław University of Science and Technology (WUST), Wrocław, Poland, in 1976, 1980, and 1991, respectively. His Ph.D. thesis was on metrological problems of scattered light application on particle size distribution investigation in dispersed solutions.

Since 1998, he has been the Head of the Chair of Electronic and Photonic Metrology, WUST, where he is currently a Full Professor. His research interests are focused on the physical and mathematical modeling in complex measurements, inverse problem, intelligent measuring devices, scattering radiation spectral and polarization analysis, multisensor data fusion, and time–frequency representations in data processing.

Prof. Mroczka is a member of SPIE and the Polish Physical Society. From 2007 to 2015, he was the President of the Committee for Metrology and Instrumentation of the Polish Academy of Science (PAS), and since 2010, he has been a Corresponding Member of PAS. He received honorary doctorates (Honoris Causa) from four Polish universities in 2014, 2017, and twice in 2019.